

Assessment of Photonic Crystal Fibers for Dispersion Factor of Different Structure

Mozhdeh Karamifard^{1*}

Abstract–Photonic crystal fibers (PCFs) are widely used in optical industries and telecommunication systems as a low dispersion and structural losses with low nonlinear coefficient. Photonic crystals are media where their refractive index distribution function is periodic or non-periodic. A manifest property of photon crystals is the presence of a band-gap in the signal transmission spectrum. Electromagnetic detection with frequency range in the band range is not prohibited. Hence, the electromagnetic waves with a frequency range in the band-gap cannot be propagated. In this paper, the dispersion property of silica core photonic crystal fibers is analyzed for three and six-ring air hole structures. It is illustrated that the six-ring air hole structure shows satisfactory results in our design. Also, considering the holes filled with concentrated silica with fluorine materials, GeO_2 , P_2O_5 , and B_2O_3 instead of air holes, it has been shown that the diffusion properties will have significant differences. The results obtained from simulations are shown by comparing with pure silica crystal.

Keywords: Photonic Crystal fiber, Dispersion characteristic, Dopant concentration, Air hole rings

1. Introduction

In 1968, Veselago introduced that the homogeneous material, with both negative permittivity (ϵ) and permeability (μ) can arise a negative index of refraction. His study showed that electric and magnetic field vectors create a set to the left of the vectors with the wave vector [1]. These homogeneous materials are known as meta-materials or left-handed meta-materials (LHM). He proposed a type of material that followed Snell's law with a negative refractive index.

The authors in [2] have observed divergence of propagation beam depending on the curvature of the dispersion surface that it was propagating in a collimator or a lens. In fact, this presentation enables the eventual fabrication of extremely compact light circuits on Si. In particular, it has been shown that photon crystal light emission with intense two- or three-dimensional modulation, even in the presence of strong multiple refractions, becomes refraction in the proximity of the photon gap band [3].

Today, PCFs have attracted a great deal of attention among societies and researchers in optics and photonics. One of the most suitable applications of PCF is the possibility of producing integrated optical devices with photons as carriers of information, which will consequently increase the speed and bandwidth in advanced telecommunication systems.

PCFs are divided into two general types: the first group is an index-guiding PCF that restricts the light by total internal reflection (TIR) between the core with a solid defect region and multiple air holes in a regular triangular lattice. The second group is used for full periodic structures to show the effect of the photonic band-gap at the operating wavelength to guide light in a low index core region [4].

In general, index-guiding PCFs are also referred micro-structured optical fibers or holey fibers, which exhibit special properties in dispersion adjustment [5]. To evaluate the dispersion properties of the PCFs, it can utilize different analytical and numerical methods with various structures. These methods are the finite difference frequency domain (FDFD) [4], scalar effective index method [6], beam propagation method (BPM) [7], the vectorial effective and improved vectorial index methods [1,8].

^{1*} **Corresponding Author** : Department of Physics, Aliabad katoul Branch, Islamic Azad University, Aliabad Katoul, Iran.

Email: mojde.karami@yahoo.com

Received: 2022.05.01; Accepted: 2022.07.13

2. Different PCF's Structure

Photonic crystal fibers are utilized in several applications like bio-medical, chemical sensing, bio-sensing, and gas sensing [9]. Moreover, some different PCFs based on sensitivity and confinement can be categorized. The sensible photonic crystals, rectangular hollow-core PCF, star shape photonic crystal, circular-pattern photonic crystal fiber, orthogonal PCF, terahertz detection PCF, and octagonal PCF are some of them. A schematic diagram of three structures of PCFs is shown in Fig.1 [10].

Also, the PCFs could be characterized as structures in where there is an intermittent variant in one, two or all three orthogonal directions of the dielectric constant and are known as one-dimensional (1D), two-dimensional (2D) and three-dimensional (3D) PCFs, respectively [11]. (Fig.2.)

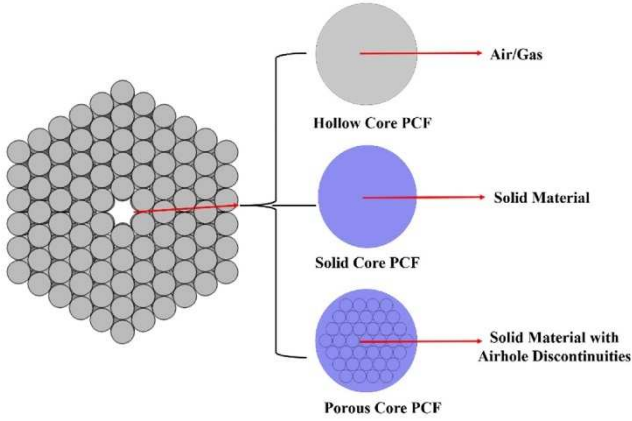


Fig.1. Schematic Diagram of three Core PCF strategies [10]

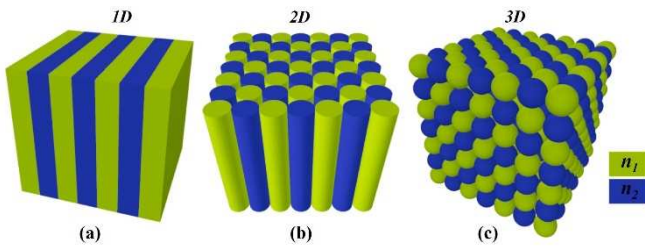


Fig.2. Graphic characterized of PCFs in, (a) 1D, (b) 2D, and (c) 3D

2.1 Designing and Modeling of PCF

PCFs have periodic dielectric components with different refractive indices that under certain conditions, cause light photon crystals to refract abnormally. This negative phenomenon is called negative refraction.

Negative refraction can be provided close to the low-frequency edge in the loss-free PCF structure, at least on two, four, or six bands. Figure 3 shows a schematic of a typical PCF with a triangular network of air-hole, where d

is the diameter of the air holes and Λ is the hole pitch. The refractive index for silica is 1.457. In the center, an air hole is removed that is forming an incomplete center with a high refractive index that acts as a fiber core [4, 12].

Some important problems in the fabrication of PCF's are the deformity in the air holes, appearance of additional holes, and trouble of unsymmetrical fiber structure. Although PCFs have many advantages over conventional single-mode fibers, the structure process of these waveguides has certain complexities that this comes from the deformation of circular holes.

3. Dispersion Properties in PCFs

The second and third equations of time-variant Maxwell's for a linear, isotropic, non-dispersive material with no source are expressed as follows [1,13]:

$$\frac{\partial \vec{H}}{\partial t} = -\frac{1}{\mu} \nabla \times \vec{E} \quad (1)$$

$$\frac{\partial \vec{E}}{\partial t} = \frac{1}{\varepsilon} \nabla \times \vec{H} - \frac{\sigma}{\varepsilon} \vec{E} \quad (2)$$

ε, μ, σ are defined as permittivity, permeability, and conductivity of the dielectric material, respectively. As we know \vec{E} and \vec{H} are respective electric and magnetic field vectors.

If we use characteristic parameters of PCF for chromatic dispersion, that is the summation of waveguide and material dispersion. For total dispersion, consisting of the material and waveguide dispersion, we can give an expression as:

$$D = -\frac{\lambda}{2\pi c} \left(2 \frac{d\beta}{d\lambda} + \frac{d^2\beta}{d^2\lambda} \right) \pi \quad (3)$$

By simplifying the above equation, we define normalized propagation constant $\beta_N = \frac{\beta}{k_0} = \frac{2\pi\beta}{\lambda}$, and then substituted this expression in equation (3) that obtained [13]:

$$D = -\frac{\lambda}{c} \left(\frac{d^2\beta_N}{d^2\lambda} \right) \pi \quad (4)$$

As we know λ and c are the wavelength and velocity of light in a vacuum, respectively, that is defined for the effective refractive index of fundamental mode $n_{eff} = \beta \left(\frac{\lambda}{2\pi} \right)$.

Then by the using Sellmeier formula, refractive index of core material is determined [14].

$$n^2(\lambda) = 1 + \sum_{i=1}^M \frac{a_i \lambda^2}{\lambda^2 - b_i^2} \quad (5)$$

Equation (5) for $M = 3$ is named the 3-term Sellmeier equation. Sellmeier formula has so many uses in the optical industry to describe and characterize the dispersion, especially in glasses and crystals. Hence, this expression for silica (with $M = 3$) can be described as:

$$n_{silica}(\lambda) = \sqrt{1 + \frac{a_1 \lambda^2}{\lambda^2 - b_1^2} + \frac{a_2 \lambda^2}{\lambda^2 - b_2^2} + \frac{a_3 \lambda^2}{\lambda^2 - b_3^2}} \quad (6)$$

The wavelength of the light is λ , and a_i and b_i are the Sellmeier coefficients. The practical values of a_i and b_i for $i=1,2,3$ are given as [15]:

$$a_1 = 0.6961663; a_2 = 0.4079426; a_3 = 0.8974794; \\ b_1 = 0.0684043; b_2 = 0.1162414; b_3 = 0.9.896161;$$

Where the wavelength λ is in nm .

By utilizing the above equations, the dispersion behaviors investigate for the two PCF's samples with different numbers of air hole rings in this study.

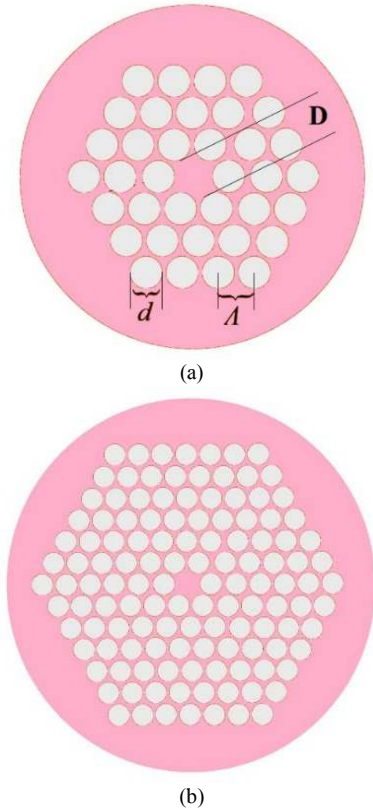


Fig.3. The design of a solid-state PCF structure, (a) 3-rings, and (b) 6-rings

4. Simulation and Results

In order to designing of the PCF structure, two schematic diagrams with three and six air hole ring arranged in the form of a triangular lattice are illustrated in Fig.3. It is shown that d , A , D are the air hole diameter, hole pitch and core diameter, respectively.

4.1 Variation of dopants concentrations

As we want to show the fibers with core and claddings, we need special glasses, which have very low losses combined to well-known refractive indices. In fiber optics, pure silica (SiO_2) with its specific dependence on the refractive index on wavelength serves as the basic material.

It is known as the refractive index can be changed by additives (dopants). This concentrated silica with dopants will be placed in the cladding instead of air-filled holes.

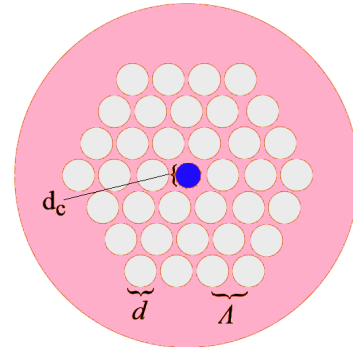


Fig.4. The solid-state PCF structure with dopant concentration

To describe this dependence on dopants concentration (D_c . In Mol%) [14]:

$$n_{Ge}(D_c) = n_{silica}(D_c) + 0.0016 * D_c \quad (7)$$

$$n_P(D_c) = n_{silica}(D_c) + 0.0009 * D_c \quad (8)$$

$$n_B(D_c) = n_{silica}(D_c) - 0.0008 * D_c + 0.00003 * D_c^2 \quad (9)$$

$$n_F(D_c) = n_{silica}(D_c) - 0.004 * D_c + 0.00015 * D_c^2 \quad (10)$$

Where $n_{silica}(D_c) = 1.457$. Also, n_{Ge}, n_P, n_B, n_F are the dispersion index of $GeO_2, P_2O_5, B_2O_3,$ and Fluorine, respectively.

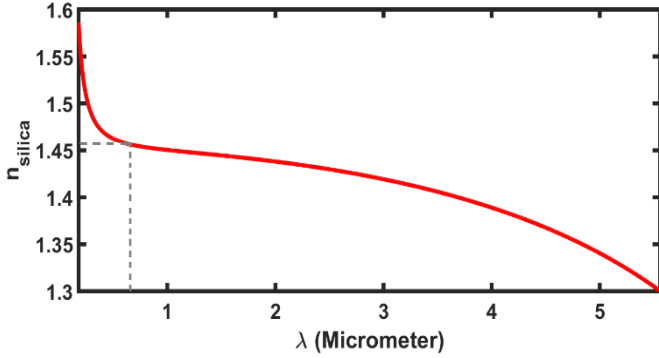


Fig.5. Dispersion behavior in silica

Result for behavior dispersion for silica is depicted in Fig. 5. The visible wavelength for silica PCFs is assumed in the referenced index as 670 nm.

Sellmeier coefficients of glasses for different dopants are given in [14]. As shown the dispersion for different dopants are very similar and only shifted by an offset. Moreover, by definition of approximated offset that is related to the concentration of materials for increasing or reducing pure silica can analyze the behavior of the dispersion index. So, the modification of the refracted indices for dopants by changing λ can be illustrated below:

$$n_{Ge}(\lambda) = n_{silica}(\lambda) + 1.4145 * 10^{-3} * d_{Ge} \quad (11)$$

$$n_P(\lambda) = n_{silica}(\lambda) + 1.6520 * 10^{-3} * d_P \quad (12)$$

$$n_B(\lambda) = n_{silica}(\lambda) - 3.7600 * 10^{-4} * d_B \quad (13)$$

$$n_F(\lambda) = n_{silica}(\lambda) - 4.6650 * 10^{-3} * d_F \quad (14)$$

Figure 6 illustrates the dispersion variation for different dopants in the wavelengths domain from 150 to 8000 nm.

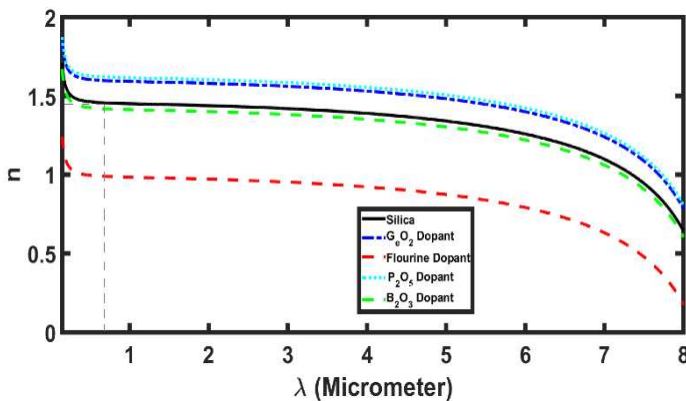


Fig.6. Dispersion behavior in glasses with different dopants

4.2 Variation of dopants concentrations

In our study, the selected PCF structure has an air hole of equal diameters $d = 0.75 \mu\text{m}$ and a hole pitch of $\Lambda = 2 \mu\text{m}$ that is arranged in three rings in the form of a triangular lattice. The core diameter is taken as $1.45 \mu\text{m}$. As for the second case, six air hole rings are considered in the cladding region as shown in Fig.3. In this case, the PCF structure is considered with the same air hole diameter of $d = 0.75 \mu\text{m}$, core diameter of $1.45 \mu\text{m}$, and a different hole pitch of $\Lambda = 1.1 \mu\text{m}$.

The chromatic dispersion spectrum (CDS) of fundamental mode for two structures in the wavelength range of 1100-2000 nm is illustrated in Fig.7. The dispersion for PCF structure with three air hole rings arrangement at 1510 nm is obtained as $-140 \frac{ps}{nm*km}$. In the second case (six air hole rings arrangement), the dispersion value is obtained $-300 \frac{ps}{nm*km}$, which approximately twice the value is obtained in the previous design of the PCF with three circular air hole rings.

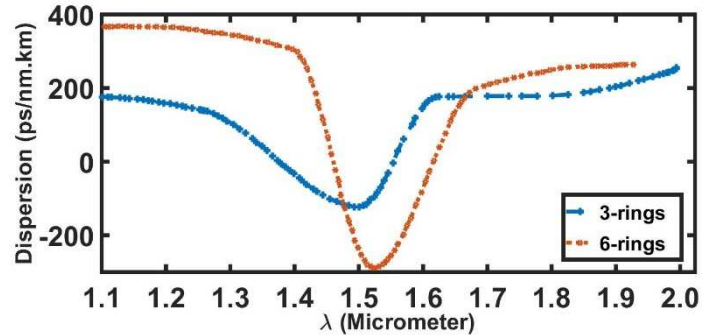


Fig.7. Dispersion spectrum of the PCFs with three and six circular air hole rings

5. Conclusion

In this paper, the 3-ring and 6-ring PCF structures are designed. Dispersion behavior for the two structures is shown that geometric changes in the PCF and in the refractive index of the substrate lead to a decrease in the dispersion of the PCFs. It is shown that with the 6-ring structure the dispersion is reduced to $-300 \frac{ps}{nm*km}$ which is almost twice that of the 3-ring structure. It is also shown that the dispersion in the PCF can be changed by dopants concentration. The refractive index of the core has been improved by additives such as germanium oxide (GeO_2).

References

- [1] S.G.J., John, et al, "Photonic crystals: molding the flow of light," *In Princeton University of Press*: Princeton, NJ, USA, 2008.
- [2] Masaya Notomi, "Negative refraction in photonic crystals," *Opt Quantum Electron*, vol.34, no.1, pp. 133-143, 2002, doi: 10.1023/A:1013300825612.
- [3] Costas M. Soukoulis, "Photonic Band Gap Materials," *Springer Science & Business Media*, vol.315, 2012, doi: 10.1007/978-94-009-1665-4.
- [4] Saitoh Kunimasa, and Masanori Koshiba, "Numerical modeling of photonic crystal fibers," *Journal of light wave technology*, vol. 23, no.11, pp.3580-3590, 2005, doi: 10.1109/JLT.2005.855855.
- [5] Raja R. Vasantha Jayakantha, et al., "Modeling photonic crystal fiber for efficient soliton pulse propagation at 850 nm," *Optics communications*, vol.283, no.24, pp.5000-5006, 2010, doi: 10.1016/j.optcom.2010.07.025.
- [6] Jes Broeng, et al., "Analysis of air-guiding photonic bandgap fibers," *Opt. Lett.*, vol. 25, no. 2, pp. 96–98, Jan, 2000, doi: 10.1364/OL.25.000096.
- [7] Fabrizio Fogli, et al., "Full vectorial BPM modeling of index-guiding photonic crystal fibers and couplers," *Opt. Express [Online]*, vol. 10, no. 1, pp. 54–59, Jan 2002, doi: 10.1364/oe.10.000054.[Available online]: <http://www.opticsexpress.org/>
- [8] Yong-Zhao Xu, et al., "A fully vectorial effective index method for accurate dispersion calculation of photonic crystal fibers," *Chinese Physics Letters*, vol.23, no.9, p.2476, 2006, doi: 10.1088/0256-307X/23/9/035.
- [9] S.Mohamed, Nizar, et al., "Comparison of Different Photonic Crystal Fiber Structure: A Review," *Journal of Physics: Conference Series, IOP Publishing (RASCC)*, vol.1717,no.1, 2021, doi:10.1088/1742-6596/1717/1/012048.
- [10] Izaddeen Kabir, Yakasai, Pg. Emeroylariffion Abas, and Feroza Begum, "Review of porous core photonic crystal fibers for terahertz waveguiding," *International Journal for Light and Electron Optics*, vol. 229, March 2021, doi: 10.1016/j.ijleo.2021.166284.
- [11] Ali Butt, Svetlana Nikolaevna Khonina, and N.L. Kazanskiy, "Recent advances in photonic crystal optical devices: A review," *Optics & Laser Technology*, vol. 142, no. 12, October 2021, doi: 10.1016/j.optlastec.2021.107265.
- [12] Mohammad Aliramezani, and Shahram Mohammad Nejad. "Numerical analysis and optimization of a dual-concentric-core photonic crystal fiber for broadband dispersion compensation," *Optics & Laser Technology*, vol.42, no.8, pp.1209-1217, 2010, doi:10.1016/j.optlastec.2010.03.012.
- [13] Faramarz E. Seraji, and Vajieh Arsang, "Analytical comparison of photonic crystal fibers for dispersion compensation with different structures using FDTD method," *Physics & Astronomy International Journal*, vol.2, no.2, pp.155-158, 2018, doi: 10.15406/paij.2018.02.00078.
- [14] Volkmar Brückner, "To the use of Sellmeier formula," *Senior Experten Service (SES) Bonn and HfT Leipzig*, vol. 42, pp. 242-250, 2011.[Available online]: <https://www.researchgate.net/profile/VolkmarBrueckner2/contributions>.
- [15] Latha, G. "Solid Core Photonic Crystal Fiber for Dispersion tailoring in Optical Tele Communication systems," *Journal of Advanced Optics and Photonics*, vol.1, no.4, pp.291-302, January 2018, doi: 10.32604/jaop.2019.06242.